J. Fluid Mech. (2015), *vol.* 772, *pp.* 361–385.
doi:10.1017/jfm.2015.161

Effect of external turbulence on the evolution of a wake in stratified and unstratified environments

Anikesh Pal[1] **and Sutanu Sarkar**[1,†]

[1]Department of Mechanical and Aerospace Engineering, University of California San Diego, CA 92093, USA

(Received 12 September 2014; revised 13 February 2015; accepted 8 March 2015; first published online 5 May 2015)

Direct numerical simulations are performed to study the evolution of a towed stratified wake subject to external turbulence in the background. A field of isotropic turbulence is combined with an initial turbulent wake field and the combined wake is simulated in a temporally evolving framework similar to that of Rind & Castro (*J. Fluid Mech.*, vol. 710, 2012*a*, p. 482). Simulations are performed for external turbulence whose initial level varies between zero and a moderate intensity of up to 7 % relative to the free stream and whose initial integral length scale is of the same order as that of the wake turbulence. A series of simulations are carried out at a Reynolds number of 10 000 and Froude number of 3. Background turbulence, especially at a level of 3 % or above, is found to have substantial quantitative effects in the stratified simulations. Turbulence inside the wake increases due to the entrainment of external turbulence, and the energy transfer through turbulent production from mean to fluctuating velocity also increases, leading to reduced mean velocity. The profiles of normalized mean and turbulence quantities in the stratified wake exhibit little change in the vertical direction but the horizontal spread increases in comparison to the case with undisturbed background. The spatial organization of the internal wave field is disrupted even at the 1 % level of external turbulence. However, key characteristics of stratified wakes such as the formation of coherent pancake vortices and the long lifetime of the mean wake are robust to the presence of fluctuations in the background. A corresponding series of simulations for the unstratified situation is carried out at the same Reynolds number of 10 000 and with similar levels of external turbulence. The change of mean and turbulence statistics is found to be weaker in the unstratified cases compared with the corresponding stratified cases and also weaker relative to that found by Rind & Castro (*J. Fluid Mech.*, vol. 710, 2012*a*, p. 482) at a similar level of external turbulence relative to the free stream and similar integral length scale. Theoretical arguments and additional simulations are provided to show that the level of external turbulence relative to wake turbulence (dissimilar between the present investigation and Rind & Castro (*J. Fluid Mech.*, vol. 710, 2012*a*, p. 482)) is a key governing parameter in both stratified and unstratified backgrounds.

Key words: stratified turbulence, turbulent flows, wakes/jets

†Email address for correspondence: ssarkar@ucsd.edu

1. Introduction

Wakes of bodies often develop in the presence of external (background) turbulence, e.g. propelled bodies, marine animals, wind turbines and particles in multiphase flow. Furthermore, the environment may be stratified in applications of interest. The effect of external turbulence on stratified wakes is poorly understood, motivating the present direct numerical simulation (DNS) study of the intermediate to far wake. We also perform simulations of unstratified wakes to provide a baseline for comparison.

Much of our current knowledge regarding the evolution of axisymmetric unstratified wakes in the presence of external turbulence is derived from work related to multiphase particulate flows. Thus, the body Reynolds number $Re = UD/\nu \approx O(100\text{–}1000)$ was small, the background turbulence integral length scale l_{int} was large relative to the body, leading to $l_{int}/D \approx O(10\text{–}100)$, and the far wake was not measured in those studies. Here, U is the free-stream velocity and $D = 2r_0$ is the body diameter. The level of external turbulence measured by the normalized root mean square (r.m.s.) of the streamwise velocity fluctuation, u'_{ext}, ranged from low to high values of u'_{ext}/U. Although we study the intermediate- to far-wake properties as well as larger bodies with larger Re and $l_{int}/D \approx O(1)$, we briefly review the literature in that different regime in the following paragraphs.

Wu & Faeth (1994) experimentally studied a sphere placed at the axis of turbulent pipe flow over the range $Re = 135\text{–}1560$ and $u'_{ext}/U = 4\,\%$, making measurements up to $x/D \approx 20$. They found that, despite being turbulent, the wake has a self-preserving behaviour with a laminar-like scaling law: the mean maximum defect velocity $U_0(x) \propto x^{-1}$ and the mean wake half-width $r \propto x^{1/2}$. The x^{-1} scaling was attributed to a constant (radially and axially) turbulent eddy viscosity and the wake spread rate was found to increase with increasing level of external turbulence. Wu & Faeth (1995) explored stronger external turbulence levels (u'_{ext}/U up to 9 %), finding that the wake decayed faster than x^{-1}, but did not further quantify the power law exponent. Bagchi & Balachandar (2004) performed DNS of flow past a sphere embedded in a frozen realization of homogeneous isotropic turbulence. The level of free-stream turbulence ($u'_{ext}/U = 10\text{–}25\,\%$) was high, and the sphere was relatively very small, so that $l_{int}/D = 52\text{–}333$ and $Re = 50\text{–}600$. The wake, simulated until $x/D = 15$, was found to exhibit $U_0 \approx x^{-1}$ decay of the mean defect velocity and a wake spreading rate that increased with the level of external turbulence, similar to Wu & Faeth (1994). Legendre, Merle & Magnaudet (2006) simulated flow past a bubble and a solid sphere placed in turbulent pipe flow. The simulations were at low $Re = 200\text{–}500$, $u'_{ext}/U = 4\,\%$ and $l_{int}/D = O(10)$. The mean wake was found to decay as $U_0 \propto x^{-2}$, faster than the wake decay in all previous studies, when the streamwise distance ($x/D > 13$ for the sphere) became sufficiently large. This effect was attributed to a crossover point when the evolving defect velocity decreased to the same order as the r.m.s. of the external turbulent fluctuations and a supporting theoretical analysis was provided. Differently from the aforementioned studies, Amoura *et al.* (2010) elected to consider external turbulence with $l_{int}/D = O(1)$, while, similarly to previous work, they considered $Re = 100\text{–}1000$. High-intensity turbulence was generated by a series of jets upstream of a water channel, and the sphere, placed on the axis of the channel, was exposed to approximately homogeneous isotropic turbulence with $u'_{ext}/U = 15\text{–}26\,\%$. The wake deficit velocity became smaller than the free-stream velocity by $x/D = 3$ and was found to subsequently exhibit $U_0 \propto x^{-2}$ scaling, much earlier than in the lower-intensity turbulence case of Legendre *et al.* (2006). Furthermore, Amoura *et al.* (2010) found that the r.m.s. of external turbulence (it did not axially decay over the

range of measurements) was the appropriate normalization velocity scale for similarity profiles and not the defect velocity.

Recently, Rind & Castro (2012*a*,*b*) studied the influence of external turbulence on intermediate- to far-wake behaviour at $Re = O(10\,000)$, higher than in previous studies. The DNS of Rind & Castro (2012*a*) adopted the temporally evolving model customary in simulations of the far wake, e.g. the planar wake by Moser, Rogers & Ewing (1998) and the axisymmetric wake by Gourlay *et al.* (2001). A background field of homogeneous isotropic turbulence was combined with an initial field having mean and turbulent velocity profiles representative of a turbulent wake, and the subsequent evolution was tracked as a function of time, a quantity that is analogous to downstream distance in the spatially evolving wake. Rind & Castro (2012*a*) simulated three cases with initial $u'_{ext}/U_0 = 0.09$, 0.17 and 0.36, corresponding to $Re \approx 10\,000$ and $u'_{ext}/U \approx 1$, 2 and 4 %. The wake deficit velocity, $U_0(t)$, was found to decay substantially faster in the cases with 2 % and 4 % external turbulence, approaching an x^{-1} law for the 4 % case. The turbulence profiles in these cases deviated from the self-similar profiles found in the pure wake. The companion experimental study by Rind & Castro (2012*b*) of the $Re = 15\,000$ wake of a disc placed in decaying grid turbulence also found that external turbulence disrupted self-similarity in turbulence profiles. The profiles of normal stresses became flatter across the wake. Turbulence levels in the far wake were found to be larger in some cases, and it was suggested that the level of external turbulence relative to the wake turbulence could be a differentiating factor. It is worth noting that external turbulence was found to affect the near wake, e.g. reduction of recirculation zone and change in drag. Direct simulations of the unstratified flow past a sphere in a computational model that includes the body have been recently performed in the turbulent regime, e.g. by Rodriguez *et al.* (2011) at $Re = 3700$. Bazilevs *et al.* (2014) compared the effect of uniform and turbulent inflow conditions on the computation of the flow over a sphere at $Re = 3700$. They reported an increase in the drag force on the sphere, dramatic reduction in the length of the recirculation bubble and significantly stronger near-wake turbulence as a consequence of adding free-stream turbulence of moderate intensity. Very-low-frequency modes, known to occur at moderate Re, were absent when free-stream turbulence was added to the inflow. The evolution of the flow into the intermediate and far wake was not possible in these body-inclusive simulations.

Stratification of the environment qualitatively changes the evolution of the intermediate to far wake, as shown by laboratory experiments on both self-propelled and towed wakes, e.g. Lin & Pao (1979), Gilreath & Brandt (1985) and Spedding, Browand & Fincham (1996*a*), as well as simulations (Ghosal & Rogers 1997; Moser *et al.* 1998; Gourlay *et al.* 2001; Dommermuth *et al.* 2002), which have recently been extended to higher Reynolds number (Brucker & Sarkar 2010; Diamessis, Spedding & Domaradzki 2011). The value of the Froude number, $Fr = U/ND$, where N is the background value of the buoyancy frequency, determines buoyancy effects. At low Fr of less than $O(1)$, the body generates internal gravity waves and the recirculation region lengthens as discussed, e.g., by Bonneton, Chomaz & Hopfinger (1993), Chomaz, Bonneton & Hopfinger (1993*a*) and Bonneton *et al.* (1996). At higher $Fr = O(1)$, corresponding to the present work, the wake is longer lived than its unstratified counterpart, has primarily horizontal motion at late time that is organized into coherent vortices, and radiates internal gravity waves. A stratified wake exhibits different stages in its evolution: a near wake (NW) where the decay rate is initially close to the unstratified case, a plateau corresponding to the onset of buoyancy effects that starts at $Nt = Nx/U \approx 2$, a non-equilibrium (NEQ) regime starting at

$Nt \approx 5$ wherein the wake decays at a rate that is slower than in the unstratified case and, finally, a quasi-2D regime where the decay rate is higher than in the NEQ regime. The NEQ regime lasts longer with increasing Re (Brucker & Sarkar 2010; Diamessis *et al.* 2011). Internal gravity waves generated by a turbulent wake are of interest and have been recently studied by Abdilghanie & Diamessis (2013) over a wide range of Re and Fr. Interestingly, the internal wave emission is prolonged to a longer time interval at high Re.

It is clear from the preceding literature survey that external turbulence may have important consequences for wakes. The evolution of a wake under the influence of a free-stream turbulence in a stratified medium has not been reported in the literature. We are thus motivated to explore the behaviour of a stratified towed wake in a disturbed ambient. The intensity of external turbulence is varied while the integral length scale remains at $l_{int}/D = O(1)$. Unstratified cases are also simulated for comparison. Several of the previous studies of unstratified wakes show a faster decay of the mean defect velocity in the presence of external turbulence. We revisit this question within the framework of wake energetics. Direct numerical simulation of the Navier–Stokes equations in a temporally evolving model, a tool that has been used in our past studies of the wake (Brucker & Sarkar 2010; de Stadler & Sarkar 2012; Pal, de Stadler & Sarkar 2013), is also employed here.

2. Problem formulation

The problem formulation and the numerical model of the towed wake are similar to those used by Brucker & Sarkar (2010). The background surrounding the turbulent wake in Brucker & Sarkar (2010) was quiescent whereas we introduce background fluctuations external to the wake in the present problem. A temporally evolving model without the body and with streamwise periodicity in the flow field is adopted as in several previous studies (Gourlay *et al.* 2001; Dommermuth *et al.* 2002; Brucker & Sarkar 2010; Diamessis *et al.* 2011). The initial velocity prescribed in the temporally evolving model has mean and r.m.s. velocity profiles taken to approximate statistics at location x_0 behind the body in the laboratory wake. The distance from the body (x in the laboratory frame) that is equivalent to clock time t in the temporally evolving model can be computed by $x = x_0 + Ut$, where U is the constant towing velocity of the body in the laboratory wake. The temporally evolving model allows simulation into the far wake without the computational cost of resolving the boundary layer at the body. It is worth noting that, once the temporal approximation is made, the actual value of U does not influence the evolution in the temporal model. The value of U determines only the temporal to spatial transformation of the statistics. Pal *et al.* (2013) showed that the results from a spatially evolving simulation match with those of a temporal simulation initialized with conditions at $x/D \approx 7$ if the inflow conditions for the spatial model match the initial conditions employed for the temporal model. The defect velocity, approximately 10 % of the body velocity, is sufficiently small at $x/D \approx 7$, allowing the temporal approximation. The initial density perturbations in the wake and the background for all the simulations are set to zero. However, if the simulations are initialized with some density perturbations of small amplitude, the statistics are not expected to show significant difference after an initial transient, based on the results of Brucker & Sarkar (2007) for a temporally evolving stratified mixing layer. The three-dimensional incompressible unsteady forms of the conservation equations for mass, momentum and density subject to the Boussinesq

approximation for buoyancy are numerically solved as discussed by Brucker & Sarkar (2010). The governing equations are non-dimensionalized using the uniform body velocity, U, and the body diameter, D.

2.1. *Towed wake initialization*

The mean and fluctuating fields are initialized with profiles that are characteristic of the NW (Uberoi & Freymuth 1970; Bevilaqua & Lykoudis 1978) for the entire domain in both the unstratified and stratified cases. The initial mean velocity profile is given by

$$\langle u_1(r)\rangle = U_0 \mathrm{e}^{(-(r/r_0)^2/2)}, \tag{2.1}$$

where U_0 is the centreline defect velocity and $r_0 = D/2$. The initial value of U_0 is taken to be 0.11, corresponding to an initial distance behind the body of $x_0/D \approx 7$. The initial velocity fluctuations are generated as an isotropic solenoidal velocity field in spectral space satisfying the following spectrum:

$$E(k) = (k/k_0)^4 \mathrm{e}^{-2(k/k_0)^2}, \tag{2.2}$$

where $k_0 = 4$. The fluctuating field is localized to the wake by multiplying it with the following function:

$$g(r) = a\left[1 + \left(\frac{r}{r_0}\right)^2\right] \mathrm{e}^{-(r/r_0)^2/2}, \tag{2.3}$$

where a is the amplitude, $r = \sqrt{x_2^2 + x_3^2}$ and $r_0 = 0.5$ is the normalization parameter. The choice of the function $g(r)$ (Dommermuth *et al.* 2002; Brucker & Sarkar 2010) is consistent with laboratory measurements of r.m.s. turbulence profiles, e.g. Bevilaqua & Lykoudis (1978). This initial fluctuating field is allowed to evolve, keeping the mean velocity profile given by (2.1) fixed until the maximum value of $\langle u_1' u_r'\rangle/K \approxeq -0.25$, ensuring that the fluctuations establish a cross-correlation that is typical of turbulent shear flow. Here, K is the turbulent kinetic energy. Azimuthal and streamwise averaging are performed to obtain the time-evolving statistics during this adjustment period.

2.2. *External turbulence*

Equation (2.2) is employed to generate the initial level of background fluctuations but, instead of using the damping function (2.3) to localize the fluctuations to the wake, a case-dependent constant value is used for the amplitude a (a is chosen so as to obtain the required ratio of u'_{ext}/U). The pre-simulations for the external turbulence are performed in a triply periodic box and allowed to evolve as an isotropic turbulent field until the required ratio of u'_{ext}/U is achieved. The background turbulence decays as time advances in the simulations.

2.3. *Calculation of statistics*

Mean statistics are computed using streamwise averaging over the computational domain length, L_1. The streamwise average in the temporally evolving model is equivalent to time averaging in the laboratory frame. The Reynolds decomposition into mean and fluctuations is

$$u_i = \langle u_i\rangle + u_i', \quad \rho = \langle\rho\rangle + \rho', \quad p = \langle p\rangle + p'. \tag{2.4a–c}$$

Case	Re	Fr	u'_{ext}/U (%)	$Re_{\lambda,ext}$	$L_{int,ext}/L_{int,cl}$	$L_{int,cl}/2r_0$
1. $EXT0_{unst}$	10 000	∞	—	—	—	4.405
2. $EXT1_{unst}$	10 000	∞	1	$\approx$41	$\approx$0.47	4.130
3. $EXT3_{unst}$	10 000	∞	3	$\approx$115	$\approx$1.21	4.118
4. $EXT4_{unst}$	10 000	∞	4	$\approx$150	$\approx$1.56	4.1
5. $EXT0_{st}$	10 000	3	—	—	—	4.405
6. $EXT1_{st}$	10 000	3	1	$\approx$41	$\approx$0.47	4.130
7. $EXT3_{st}$	10 000	3	3	$\approx$115	$\approx$1.21	4.118
8. $EXT4_{st}$	10 000	3	4	$\approx$150	$\approx$1.56	4.1

TABLE 1. Parameters of the unstratified and stratified wake simulations. The level of external turbulence is systematically varied from zero to 4 % of the free-stream mean velocity. The ratio of the initial integral length scale of the external turbulence, $L_{int,ext}$, to that of the wake turbulence at the centreline, $L_{int,cl}$, also increases while remaining $O(1)$. The microscale Reynolds number of the external free-stream turbulence, $Re_{\lambda,ext} = (20/3)(k^2/\epsilon\nu)^{1/2}$, is moderate. Here, k and ϵ are the turbulent kinetic energy and dissipation rate respectively. All simulations were performed with $N_1 = 2048$, $N_2 = 512$ and $N_3 = 384$ grid points in the x_1 (streamwise), x_2 (spanwise) and x_3 (vertical) directions respectively. Here, $L_1 = 81.92$, $L_2 = 18.84$ and $L_3 = 13.72$ are the computational domain lengths normalized by the body and excluding the sponges.

Statistics in the stratified wake are a function of time (t) as well as the spanwise (x_2) and vertical (x_3) directions. Although statistics in the unstratified wake are a function of the radial coordinate (r) and t, we do not present profiles as a function of r and, therefore, do not perform additional azimuthal averaging.

2.4. *Simulation parameters*

The parameters of the different cases are summarized in table 1. The intensity, u'_{ext}/U, of the external fluctuations is varied between 0 and 4 % in both unstratified and stratified ($Fr = 3$) situations. The ratio of the initial integral length scale of the external fluctuations ($L_{int,ext}$) to the corresponding value at the centreline ($L_{int,cl}$) is $O(1)$, as shown in table 1. The initial value of the microscale Reynolds number is moderate, with a value of $Re_\lambda = 150$ at the highest turbulence intensity of 4 %. For the stratified cases, the initial density field has a linear gradient in the vertical direction corresponding to $Fr = 3$ ($Fr = U/ND$, $N^2 = -(g/\rho_0)(\partial\rho/\partial x_3)$, where $\rho_0 = 1$ is the reference density) without superposed fluctuations. Approximately 400 million equispaced grid points are used for the simulations. The simulations are designed with a resolution of $\Delta x_i/\eta < 4$ for all the cases. Here, η is the Kolmogorov length scale calculated as $\eta \equiv (Re^3\varepsilon)^{-1/4}$, with ε denoting the non-dimensional turbulent dissipation rate defined by $\varepsilon \equiv (2/Re_0)\langle s'_{ij}s'_{ij}\rangle$, where $s'_{ij} = ((\partial u'_i/\partial x_j) + (\partial u'_j/\partial x_i))/2$.

The external turbulent field (§ 2.2) is combined with the towed wake (§ 2.1) in the outer region of the wake which, following Redford & Coleman (2007), is taken to be the region where the mean velocity of the towed wake is less than 5 % of the maximum defect velocity. The combined field is allowed to adjust for a few time units to smear out the gradients that are initially generated at the interface between the two fields. Figure 1(*a*) shows the initial radial profiles of $u_{1,rms}$ after the adjustment period. The external values of the r.m.s. velocity fluctuation vary from small to substantial fractions of the corresponding values at the wake centreline. Profiles of the Taylor microscale Reynolds number, $Re_{\lambda,ext}$, are shown in figure 1(*b*). In the stratified cases,

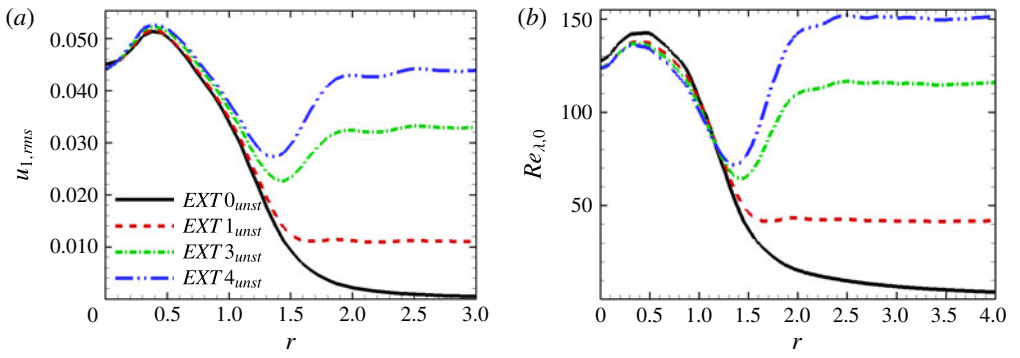

FIGURE 1. (Colour online) (*a*) Initial profile of r.m.s. velocity, $u'_{1,rms}$. (*b*) Initial profile of Taylor microscale Reynolds number, Re_λ.

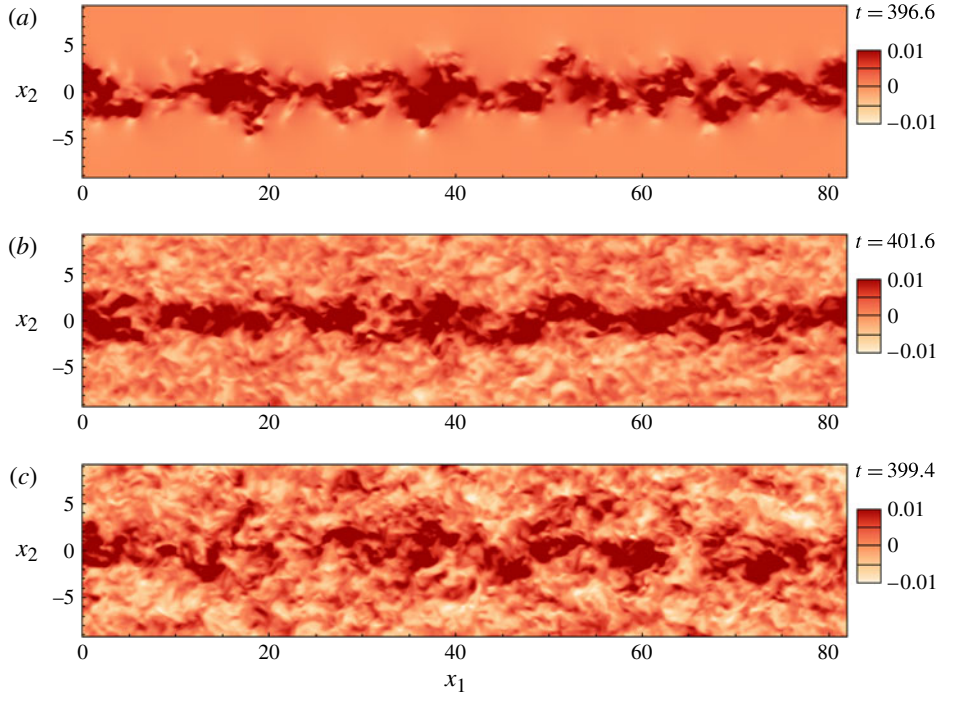

FIGURE 2. (Colour online) Instantaneous streamwise velocity at time $t \approx 400$ in the unstratified cases: (*a*) $EXT0_{unst}$, (*b*) $EXT1_{unst}$ and (*c*) $EXT4_{unst}$.

the combined field undergoes a further buoyancy adjustment time during which the density fluctuations are allowed to increase from their initial zero value.

3. Visualization

The qualitative effects of a turbulent background on the spatial organization of the flow are examined through visualizations of velocity and vorticity. It will be shown below that external turbulence disrupts some features of the organization of

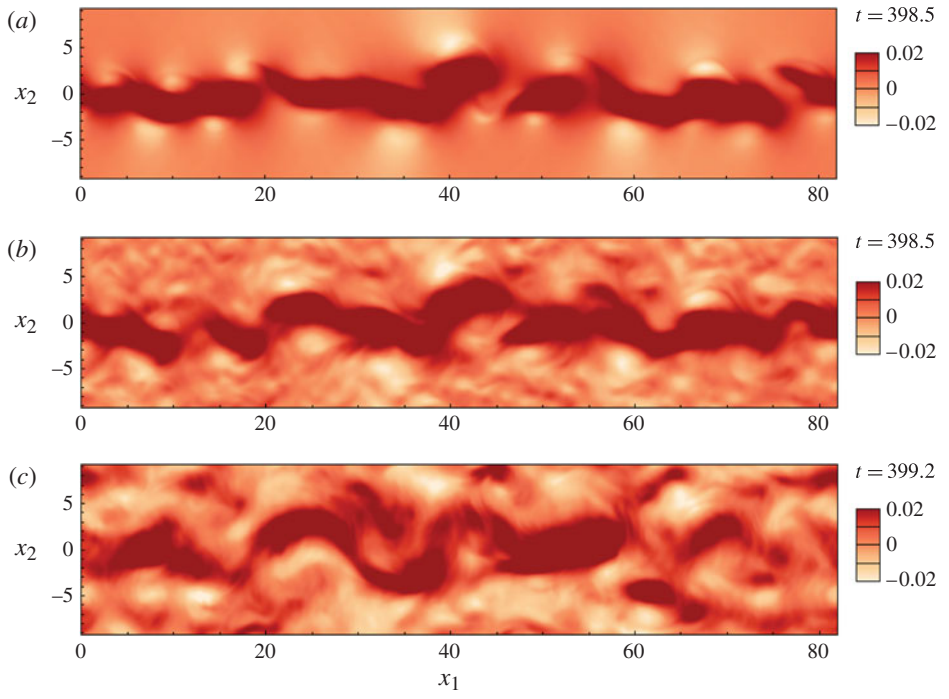

FIGURE 3. (Colour online) Instantaneous streamwise velocity at $t \approx 400$ ($Nt \approx 133$) in the stratified cases at the centre plane ($x_3 = 0$): (*a*) $EXT0_{st}$, (*b*) $EXT1_{st}$ and (*c*) $EXT4_{st}$.

the stratified wake, e.g. internal gravity waves, but not others, e.g. coherent pancake eddies.

The evolutions of the instantaneous wake velocity for the unstratified cases and the stratified cases are shown in figures 2 and 3 respectively. The streamwise velocity for $EXT0_{unst}$ (figure 2*a*) shows a recognizable wake pattern. Similarly, the case with 1 % external turbulence in figure 2(*b*) also displays an identifiable wake pattern. However, when the external turbulence level increases to 4 %, the wake core is significantly modified by entrainment of background fluid with small-scale turbulence, and it becomes more difficult to distinguish the wake from the background in figure 2(*c*). The evolution of the wake under the influence of 1 % free-stream turbulence in a stratified fluid (figure 3*b*) is similar to the stratified case without background turbulence (figure 3*a*). It is noticeable that the wake of case $EXT4_{st}$ evolves into large coherent structures whereas the wake of case $EXT4_{unst}$ has a plethora of small-scale structures. The external turbulence in case $EXT4_{st}$ becomes organized into larger-scale coherent patches by buoyancy, so that entrainment of external fluctuations into the wake at later time does not lead to additional small-scale fluctuations in the wake. Therefore, although the 4 % external turbulence diminishes the prominence of the stratified wake relative to the background with respect to the 'clean' case, it does not disrupt the stratified wake core as much as in the corresponding unstratified case.

External turbulence disrupts the well-known pattern of internal waves. Figure 4 shows visualizations of the horizontal vorticity ω_1 in an x_2–x_3 cross-section of the flow. At $t \approx 60$, case $EXT0_{st}$ without background fluctuations shows the propagation of internal gravity waves into the background. Even the case with a low level

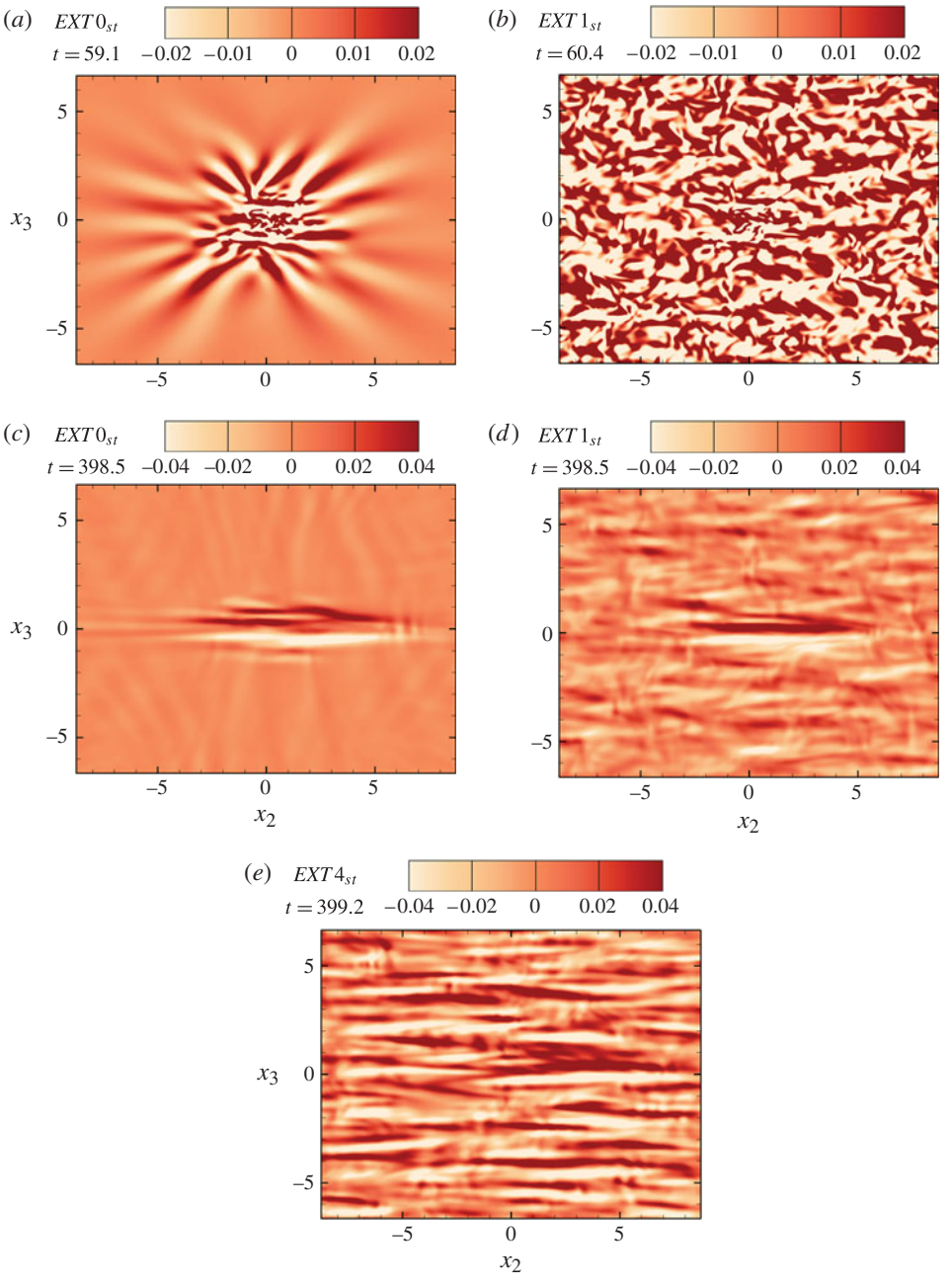

FIGURE 4. Snapshots of instantaneous ω_1 in a vertical–lateral cross-section of the stratified cases. (*a*,*b*) Comparison of the fields at $t \approx 60$ between the undisturbed background case (*a*) and the case with 1 % external turbulence (*b*). (*c*,*d*) The same comparison at a later time, $t \approx 400$. (*e*) Snapshot corresponding to 4 % external turbulence.

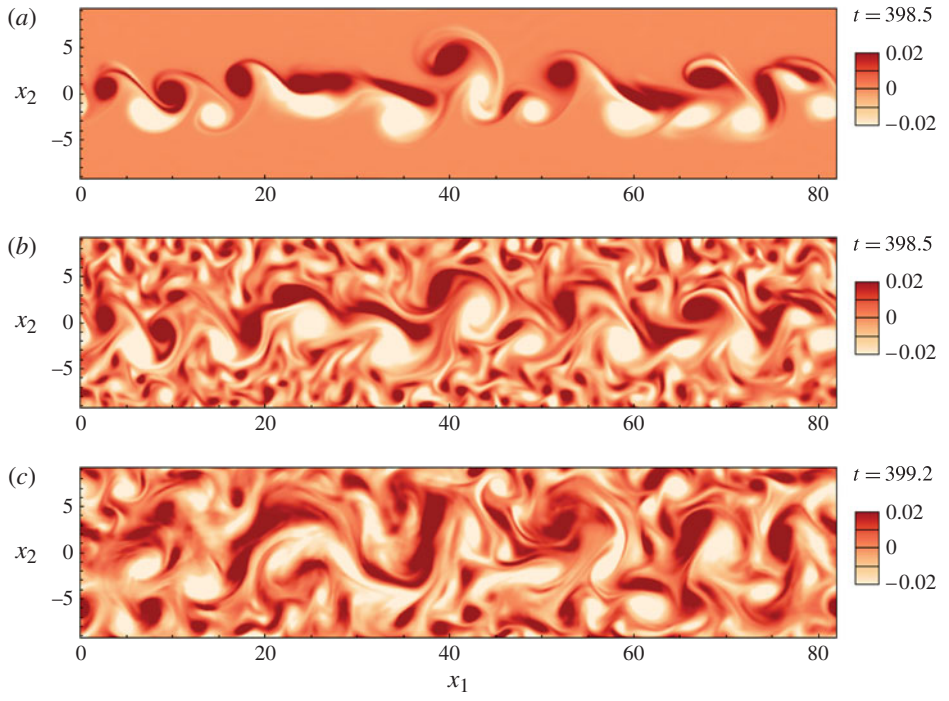

FIGURE 5. Vertical vorticity at a horizontal cross-section in the stratified cases: (*a*) $EXT0_{st}$, (*b*) $EXT1_{st}$ and (*c*) $EXT4_{st}$ at $t \approx 398$ ($Nt \approx 133$).

of 1 % background turbulence (figure 4*b*) exhibits a chaotic pattern of streamwise vorticity with almost no suggestion of wake-generated internal waves. At a later time $t \approx 398$, $EXT0_{st}$ displays the formation of multiple layered structures (figure 4*c*), which are a defining characteristic of pancake eddies in strongly stratified vortical flows. In contrast to the barely discernible wave pattern at early time, case $EXT1_{st}$ at $t \approx 398$ shows multiple layered structures similar to those of $EXT0_{st}$, revealing the presence of a wake. Case $EXT4_{st}$ also shows the formation of layered structures at $t \approx 398$ (figure 4*c*); however, the external turbulence also evolves into similar layered structures, making it difficult to recognize the wake.

The organization of horizontal motion into coherent eddies is a distinguishing feature of stratified flows. Figure 5 shows snapshots of the vertical vorticity ω_3 in the x_1–x_2 plane for the different stratified cases. Large coherent vortices emerge, as can be seen at $t = 398$ for case $EXT0_{st}$ (figure 5*a*). Case $EXT1_{st}$ shown in figure 5(*b*) also displays coherent vortices at this time, similar to case $EXT0_{st}$. These coherent structures are surrounded by the smaller vortices formed by the external turbulence. These small vortices interact and distort the primary vortex structure of the wake. As the external turbulence intensifies (figure 5*e*), the background fluctuations evolve into larger vortices that interact with the wake and significantly distort the coherent structures in the wake core. In the unstratified case, the wake does not evolve into coherent horizontally eddying motion. Therefore, it becomes difficult to distinguish the wake at $t \approx 400$ from the background in snapshots of the vertical vorticity, even with 1 % external turbulence (not shown here).

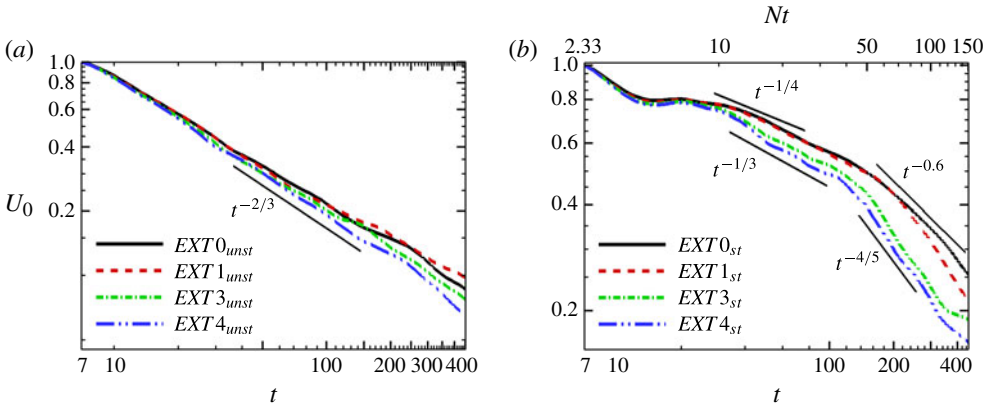

FIGURE 6. (Colour online) Centreline defect velocity normalized by the initial value: (*a*) unstratified cases and (*b*) stratified cases.

4. Mean flow characteristics

Figure 6(*a*,*b*) shows the evolution of the mean centreline defect velocity $U_0(t)$ for the unstratified and stratified cases respectively. The unstratified cases in figure 6(*a*) exhibit a t^{-n} power law with the classical $n=-2/3$ power law beyond $t\approx 25$. The virtual origin, t_0, of the self-similar law, $U_0=A(t-t_0)^{-2/3}$, is obtained by the intercept of a linear fit to $U_0^{-3/2}(t)$ (plotted in linear–linear scale) with the t-axis. The velocity, thus plotted, exhibits an excellent fit in the case without external turbulence to a straight line that has $t_0\approx 10$, while the other cases show adequate straight line fits with non-zero values for t_0. The initial conditions are known to influence the existence of self-similar behaviour and the virtual origin of the power laws. For instance, Redford, Castro & Coleman (2012) compare two very different initial conditions (equispaced vortex rings versus low-level broadband noise superposed on a mean velocity profile) and find that each case exhibits self-similar power laws relatively early ($t_0\approx 60$ in the vortex ring case) in the mean defect velocity and half-width with the expected exponents, but the thickness growth rates are different between the two initializations for a long period before eventually approaching a common, possibly universal, value. The surprisingly small value of $t_0\approx 10$ in the present simulations may be due to the precursor adjustment period where the fluctuations are allowed to develop a correlation coefficient of $\langle u_1' u_r'\rangle/K\cong -0.25$, typical of shear flows, before evolving the wake.

The effect of external turbulence on the evolution of the centreline mean defect velocity is weak in the unstratified cases relative to the stratified situation (figure 6*b*), where U_0 is reduced by almost a factor of 2 at $t=300$ in case $EXT4_{st}$ with 4 % external turbulence compared with the $EXT0_{st}$ case. In case $EXT1_{st}$, the mean defect velocity evolves similarly to $EXT0_{st}$ until $Nt\approx 70$ when it deviates. Increasing the intensity of the external turbulence to 3 % and 4 % results in a much earlier ($Nt\approx 10$) deviation of the defect velocity towards smaller values relative to $EXT0_{st}$. It should be noted that $Nt\approx 10$ is approximately the same buoyancy time period where the accelerated collapse phase occurs, as reported by Bonnier & Eiff (2002) and Brucker & Sarkar (2010). At $Nt\approx 10$, the wake starts to preferentially expand in the horizontal direction. Background turbulence enhances the expansion leading to values of the defect velocity that are smaller relative to the case with quiescent background. The nominal decay rates are found to follow an approximate scaling of $t^{-1/3}$ during

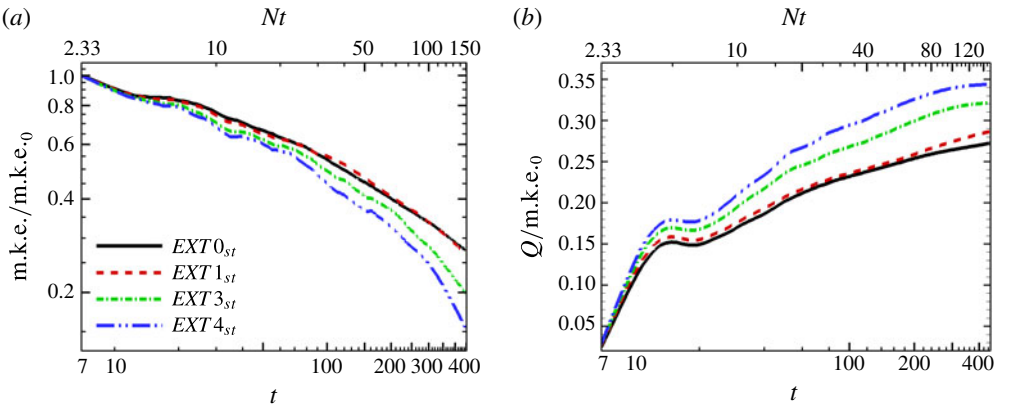

FIGURE 7. (Colour online) (*a*) Integrated mean kinetic energy in the stratified cases and (*b*) cumulative integral of turbulent production normalized by the initial integrated mean kinetic energy in the stratified cases.

the period $10 < Nt < 50$ for $EXT3_{st}$ and $EXT4_{st}$. During the period $50 < Nt < 120$, all the cases with external turbulence follow an approximately $t^{-4/5}$ scaling for the decay rate of the defect velocity.

It is worth emphasizing that, although the magnitude of U_0 under the influence of the external turbulence is quantitatively reduced with respect to the stratified wake with undisturbed background, the qualitative effects of buoyancy on the evolution of the defect velocity are unaltered. The different stages of the evolution of U_0 are preserved, i.e. we find an NW where the decay rate is initially close to the unstratified case, a plateau corresponding to the onset of buoyancy effects, an NEQ regime where the wake decays at a rate that is slower than in the unstratified case and, finally, a quasi-2D regime where the decay rate is higher than in the NEQ regime.

The evolution of the mean kinetic energy, m.k.e. $\equiv \langle u_i \rangle \langle u_i \rangle / 2$, is given by

$$\frac{\mathrm{D(m.k.e.)}}{\mathrm{D}t} = -P + \overline{B} - \overline{\varepsilon} - \frac{\partial T_i}{\partial x_i}, \tag{4.1}$$

where P is the production of turbulent kinetic energy, $\overline{B}$ is the buoyancy flux associated with mean fields, $\overline{\varepsilon}$ is the viscous dissipation rate of the mean velocity and T_i is the transport of the m.k.e. Figure 7(*a*) shows that the area-integrated m.k.e., similarly to the centreline defect velocity, also exhibits enhanced decay in the presence of external turbulence. The area of integration is taken to be the half-width region so as to focus on the wake core. To understand the faster decay of the defect velocity and the m.k.e. under the influence of higher intensities of external turbulence, it is helpful to note the following characteristics of the area-integrated (4.1): the production of the turbulent kinetic energy, P, is the dominant term, the value of P is positive here, as in most turbulent shear flows, and the negative sign preceding P implies the loss of m.k.e. to turbulence. The effect of the turbulent production on the mean wake is presented in figure 7(*b*) by calculating the cumulative integral of production over the half-width,

$$Q = \int_0^t \int_C P \mathrm{d}C \mathrm{d}t, \tag{4.2}$$

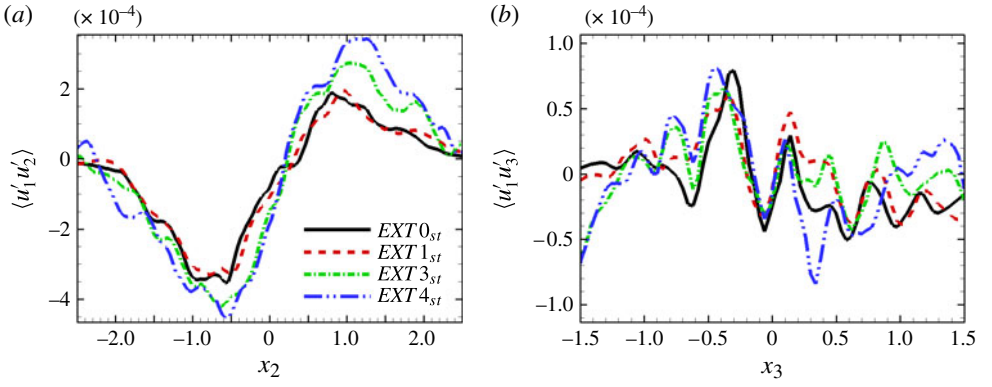

FIGURE 8. (Colour online) Reynolds stress at $t \approx 30$ in the stratified cases: (*a*) $\langle u_1' u_2' \rangle$ corresponding to motion in horizontal planes and (*b*) $\langle u_1' u_3' \rangle$ corresponding to motion in vertical x_1–x_3 planes.

normalized by the initial area-integrated value of the m.k.e. Figure 7(*b*) shows that, as the intensity of the external turbulence increases, the fraction of initial m.k.e. removed by turbulent production diverges from the quiescent free-stream case. The higher values of this fraction for $EXT3_{st}$ and $EXT4_{st}$ signify that the external fluctuations enhance the turbulent production term in (4.1), thereby removing energy from the m.k.e. reservoir faster than in the case with undisturbed background. This leads to the faster mean wake decay in the presence of external turbulence, as shown by figures 7(*a*) and 6(*b*).

5. Fluctuating flow characteristics

Changes to the mean velocity are accompanied by changes to the turbulence characteristics, e.g. turbulence levels inside the wake are enhanced, horizontal profiles tend to be flatter and vertical profiles are unchanged in shape. Figure 8(*a*,*b*) shows Reynolds shear stress profiles at $t \approx 30$. The profiles of $\langle u_1' u_2' \rangle$ for $EXT0_{st}$ and $EXT1_{st}$ are similar. However, the cases with 3 % and 4 % external turbulence exhibit higher values of Reynolds shear stress associated with horizontal motion, as illustrated by figure 8(*a*). As the intensity of the external turbulence increases to 3 % or 4 %, the entrainment of external turbulence from the horizontal direction into the wake also increases, resulting in the increase of $\langle u_1' u_2' \rangle$. In contrast, the Reynolds shear stress $\langle u_1' u_3' \rangle$, corresponding to vertical motion, does not show clear differences among the different cases, consistent with the effect of external turbulence being more prominent on horizontal motion, as was seen in the preceding sections. The Reynolds shear stress, $\langle u_1' u_2' \rangle$, in the wake is correlated to the horizontal mean velocity gradient, $\partial \langle u \rangle_1 / \partial x_2$ (not shown here), similarly to the findings of Meunier & Spedding (2006) and de Stadler & Sarkar (2012), irrespective of background turbulence.

The pointwise turbulent kinetic energy, t.k.e. $= \langle u_i' u_i' \rangle / 2$, is obtained by streamwise averaging and is a function of x_2 and x_3. Profiles of K along the horizontal and vertical centrelines are shown in figures 9–10 at two different times. At $t \approx 60$, the t.k.e. profile of the $EXT1_{st}$ wake is similar to that of the $EXT0_{st}$ wake (figures 9*a* and 10*a*) except at the edges of the wake. With the increase in the intensity of the external turbulence to 3 % and 4 %, the t.k.e. in the wake core exhibits a higher

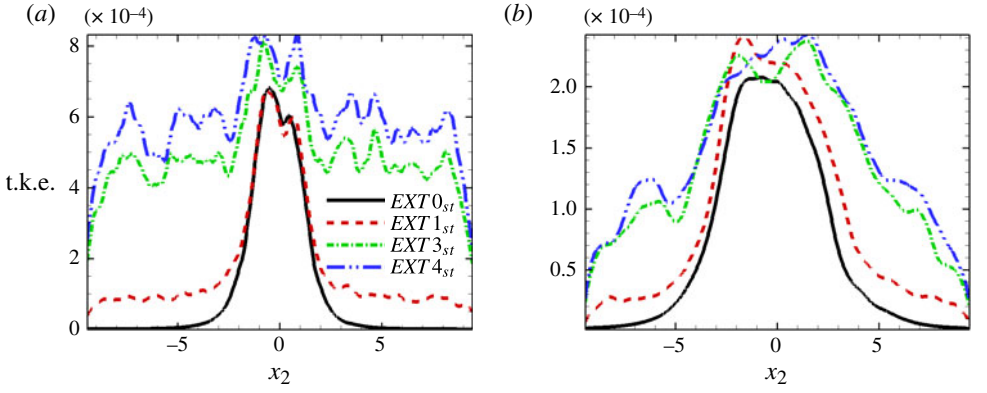

FIGURE 9. (Colour online) Turbulent kinetic energy at the central line in the horizontal direction for the stratified cases: (*a*) $t \approx 60$ and (*b*) $t \approx 300$.

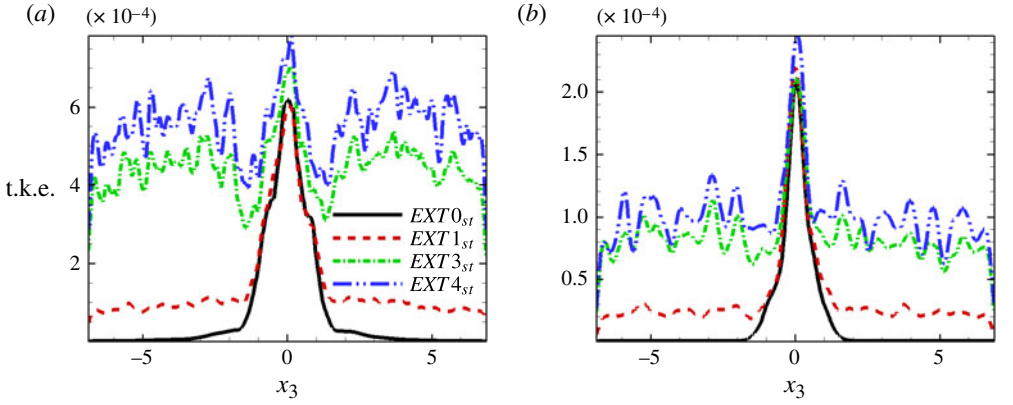

FIGURE 10. (Colour online) Turbulent kinetic energy at the central line in the vertical direction for the stratified cases: (*a*) $t \approx 60$ and (*b*) $t \approx 300$.

value compared with case $EXT0_{st}$. Analysis of the t.k.e. budget, discussed later, shows that shear production is enhanced and that turbulent transport from the wake to the background is reduced in the presence of external turbulence, thus keeping the t.k.e. larger in the wake core. As time advances, the horizontal expansion of the wake is significantly higher for the cases with 3 % and 4 % external turbulence compared with cases $EXT0_{st}$ and $EXT1_{st}$ (figure 9*b*). The vertical spread of the wake is strongly suppressed by buoyancy in all cases and is relatively unaffected by the background turbulence. Furthermore, in contrast to the horizontal profiles, the vertical profiles show a distinct break between the almost uniform level of background turbulence and the higher level of wake turbulence, reinforcing the notion that buoyancy strongly inhibits vertical entrainment in the cases simulated here.

Figure 11(*a*,*b*) shows the time evolution of t.k.e., the area-integrated turbulent kinetic energy, normalized by its initial values for the unstratified and stratified cases respectively. The area of integration is again taken to be the half-width region so as to focus on the wake core. The integrated t.k.e. in the unstratified situation (figure 11*a*) increases until $t \approx 18$ at a similar rate among all cases, then commences to decay

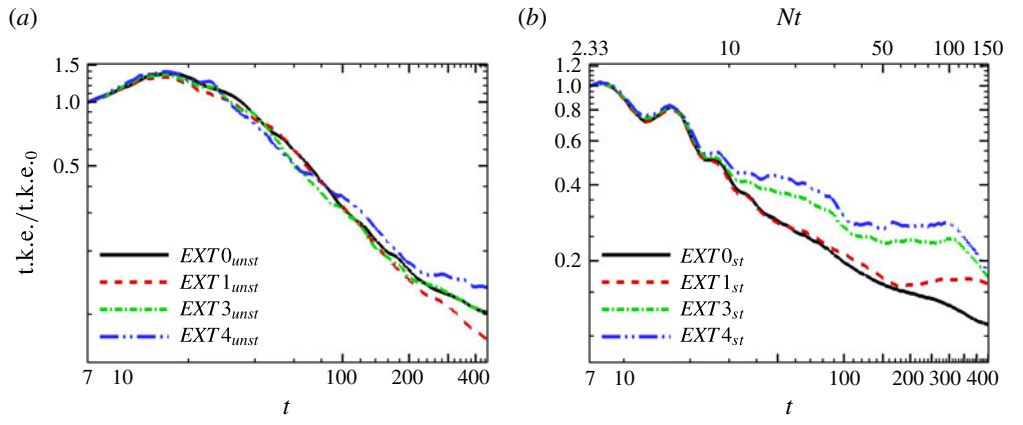

FIGURE 11. (Colour online) Turbulent kinetic energy integrated over the half-width: (*a*) unstratified cases, (*b*) stratified cases.

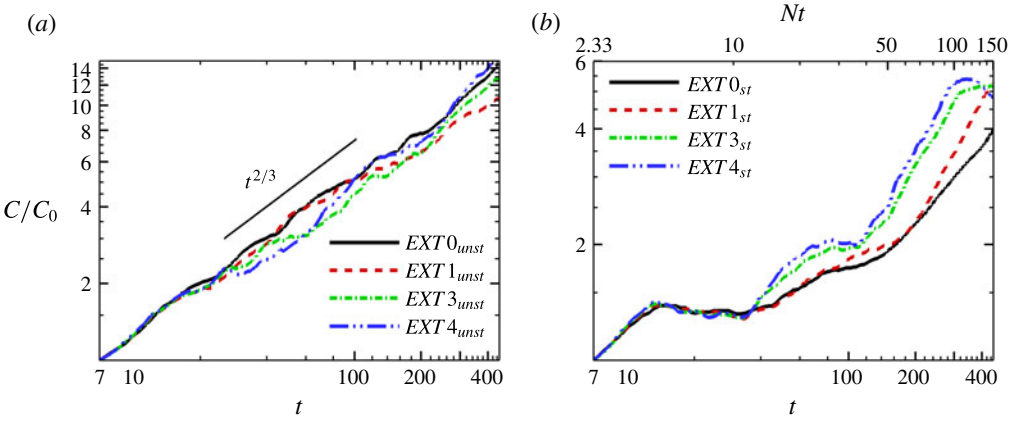

FIGURE 12. (Colour online) Half-width area: (*a*) unstratified cases, (*b*) stratified cases.

after $t \approx 18$ with a rate that is again similar among the cases until $t \approx 200$ when some differences appear among cases. In the stratified cases (figure 11*b*), the integrated t.k.e. evolves similarly until $Nt \approx 10$ for all the cases. The oscillations observed in the evolution of the t.k.e. are due to the oscillations in the buoyancy flux responsible for reversible exchange between the potential and kinetic energy. Subsequently, the t.k.e. for case $EXT1_{st}$ continues to decay at a rate similar to that of $EXT0_{st}$, but the decay of the t.k.e. slows down as the intensity of the background turbulence is increased to 3 % and 4 %. The reason for this behaviour is the enhanced horizontal entrainment of the fluctuating energy from outside the wake, which is also consistent with the formation of larger vortices in the NEQ regime in these cases, as was seen in the earlier section on visualizations. The increased level of t.k.e. in the cases with higher external turbulence level is also consistent with the increased level of turbulent production, P.

Figure 12(*a*,*b*) represents the evolution of the half-width area for the unstratified and stratified cases respectively. Case $EXT0_{unst}$ shows a scaling of approximately $t^{2/3}$ for the half-width area, which is in agreement with a scaling of $t^{-2/3}$ for the defect

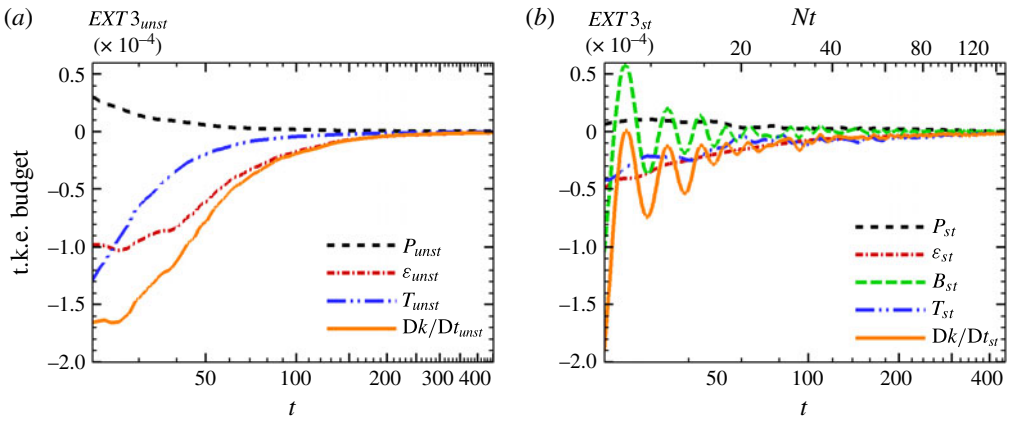

FIGURE 13. (Colour online) Turbulent kinetic energy budget integrated over the half-width for the cases (*a*) $EXT3_{unst}$ and (*b*) $EXT3_{st}$.

velocity. The cases with the external turbulence also follow an approximately similar scaling. In the stratified cases, the half-width area increases similarly to the unstratified cases until $Nt \approx 5$. During $5 < Nt < 10$, there is a plateau in the half-width area indicative of the suppression of entrainment in the vertical direction due to the effect of buoyancy. Beyond $Nt \approx 10$, entrainment resumes in the horizontal direction and the half-width continues to grow. Enhanced horizontal entrainment in the presence of background turbulence leads to an increase in the half-width area for the cases $EXT3_{st}$ and $EXT4_{st}$ compared with $EXT0_{st}$ and $EXT1_{st}$.

The characteristics of external turbulence relative to wake turbulence during the evolution have been examined (but not plotted here) in the unstratified cases. The external and centreline values of the t.k.e. decay initially at different rates but eventually decay at a similar rate of approximately $t^{-1.4}$. The ratio t.k.e.$_{ext}$/t.k.e.$_{cl}$ approaches an approximately constant value in each case which varies among cases (from 1.25 in $EXT1_{unst}$ to 2.5 in $EXT4_{unst}$). The relative evolution of the integral length scales of turbulence is also of interest. We find that the integral length scales of both wake turbulence and external turbulence decrease during an initial transient, $t < 50$. Interestingly, as a result of the initial transient, the value of $l_{int,ext}/l_{int,cl}$, which initially varied between 0.47 ($EXT1_{unst}$) and 1.56 ($EXT4_{unst}$) among cases, approaches the value of unity. Later, the length scales increase with time and there is some difference in the background/wake turbulence length scale ratio among cases at late times, e.g. $l_{int,ext}/l_{int,cl}$ is $\sim$0.5 in $EXT1_{unst}$ and $\sim$1 in $EXT4_{unst}$.

6. Turbulent kinetic energy budget

The evolution of the turbulent kinetic energy, t.k.e. $= \langle u_i' u_i' \rangle / 2$, is given by

$$\frac{\mathrm{D(t.k.e.)}}{\mathrm{D}t} = P + B - \varepsilon - \frac{\partial T_i'}{\partial x_i}, \tag{6.1}$$

where P is the production, B is the buoyancy flux, ε is the turbulent dissipation rate and T_i' is the transport term. The evolution of t.k.e., the turbulent kinetic energy integrated over the half-width area, was shown previously. The balance of terms resulting in the evolution of t.k.e. is of interest and has been obtained by integration

over the half-width area of terms in (6.1). Figure 13(*a*) illustrates the balance for the unstratified case with 3 % external turbulence. The production, P, is initially large, but soon the spatial transport of t.k.e., $\partial T_i'/\partial x_i$, and dissipation, ε, dominate. By $t = 100$, the turbulent dissipation rate dominates all other terms and is balanced by the time-derivative term. The main differences in the stratified case are as follows: the reduced magnitude of all the terms, the reduced value of shear production relative to other terms, the transport term remains comparable to the turbulent dissipation term beyond $t = 100$ and the presence of the buoyancy term, B, which exhibits large temporal oscillations between positive and negative values making it comparable to the other terms in the balance for $t < 50$. The oscillation of B also leads to an oscillatory modulation of the D(t.k.e.)/Dt term in the balance. However, the time-integrated value of the buoyancy flux is much smaller than the corresponding value for turbulent dissipation.

Figures 14(*a*) and (*b*) show the t.k.e. shear production components, P_{12} and P_{13}, respectively, integrated over the half-width area and normalized by their initial values. Here, P_{12} is associated with horizontal mean shear, $\partial\langle U_1\rangle/\partial x_2$, and P_{13} with vertical mean shear, $\partial\langle U_1\rangle/\partial x_3$. The component P_{12} decreases at a similar rate for all the cases until $Nt \approx 9$. During the period $9 < Nt < 20$, P_{12} is enhanced in cases $EXT3_{st}$ and $EXT4_{st}$ relative to the other cases. The increased levels of P_{12} in cases $EXT3_{st}$ and $EXT4_{st}$ are consistent with the enhancement of Reynolds shear stress in these cases shown earlier in figure 8(*a*). An increase in P_{12} also signifies an increase in the extraction of energy from the mean velocity field, leading to the faster decay of the mean velocity that was noted earlier for the stratified cases with background turbulence. The evolution of P_{13} shows little difference among cases. The P_{12} component remains positive at all times whereas P_{13} decreases to a negative value at $Nt \approx 4$, indicating a transfer of energy from the fluctuating modes to the mean streamwise velocity. The component P_{13}, after achieving a minimum value at $Nt \approx 6$, evolves towards zero in all cases.

The horizontal and vertical components of the transport of the t.k.e., again integrated over the half-width area and normalized by their initial values, are presented in figures 14(*c*) and (*d*), respectively. The sum of the components, i.e. the divergence of the transport term, is always negative when integrated over the half-width region, which implies that the direction of net transport of turbulence is from the core of the wake to its lateral and vertical flanks. The background turbulence in the simulated cases is not strong enough to change this typical feature of turbulent shear flows. Background turbulence has little effect on the contribution of the vertical gradient (figure 14*d*), integrated over the half-width area. However, turbulent transport by horizontal gradients (figure 14*c*) is diminished in cases $EXT3_{st}$ and $EXT4_{st}$. Entrainment of background fluctuations increases the turbulence level at the outer flanks of the wake (figure 9), reducing the net turbulent transport from the wake core to the flank.

Figure 14(*e*) compares the turbulent dissipation rate, integrated over the half-width area and normalized by the initial value, among the various stratified cases. During the early evolution until $Nt \approx 10$, case $EXT0_{st}$ exhibits values that are higher than the cases with external turbulence. Beyond $Nt \approx 10$, the dissipation rate for the cases with 3 % and 4 % external turbulence is larger relative to the cases $EXT0_{st}$ and $EXT1_{st}$. The enhanced values of ε in cases $EXT3_{st}$ and $EXT4_{st}$ are consistent with the entrainment of external fluid with energetic smaller-scale fluctuations. Case $EXT1_{st}$, due to lower intensity of external turbulence, shows little change with respect to $EXT0_{st}$.

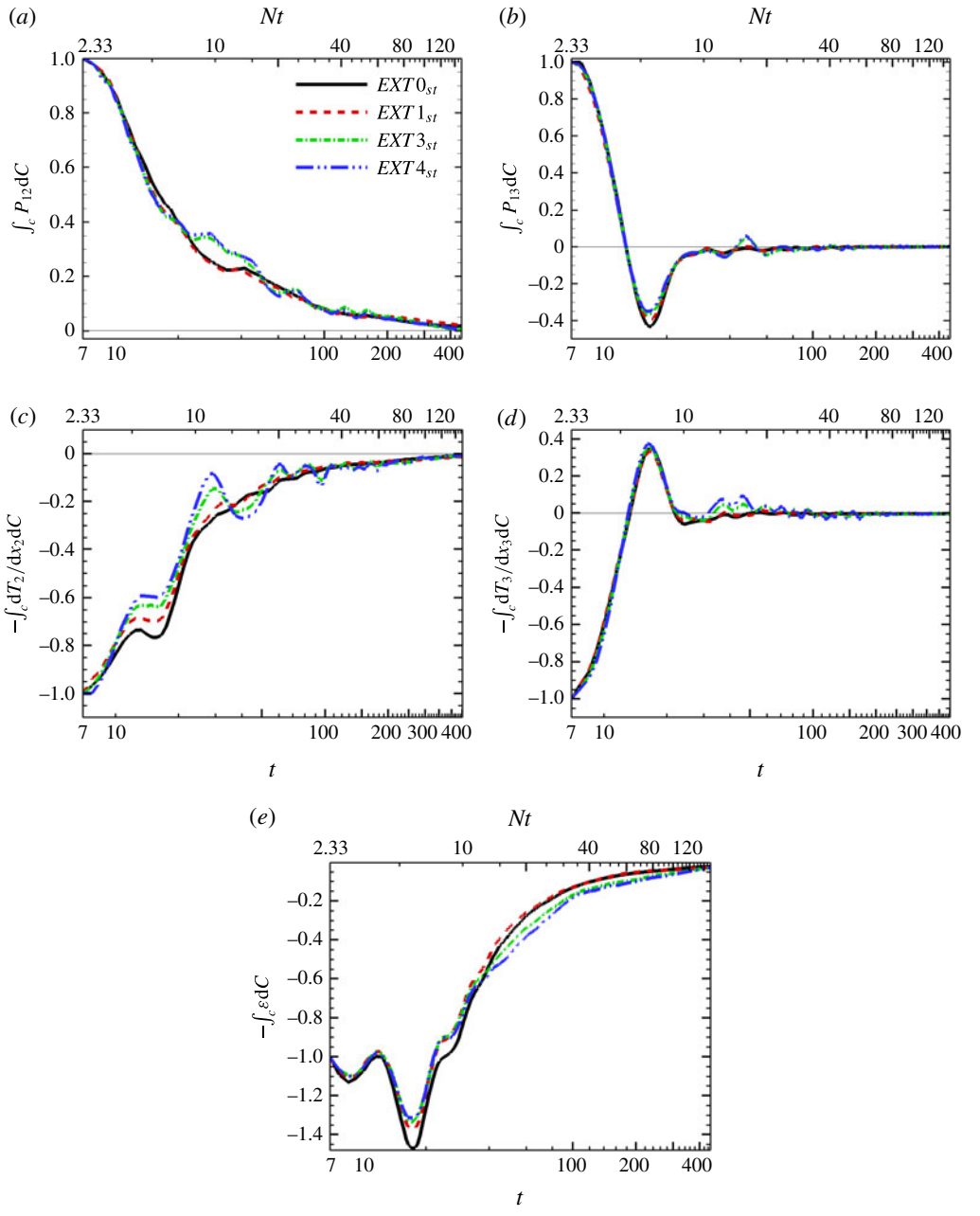

FIGURE 14. (Colour online) *TKE* Budget terms for the stratified cases integrated over the half-width: (*a*) horizontal production component, (*b*) vertical production component, (*c*) horizontal transport component (*d*) vertical transport component and (*e*) dissipation.

7. Discussion of the evolution of mean wake velocity

In the present simulations of the unstratified wake, the defect velocity, $U_0(t)$, decays at a rate similar to the classical $t^{-2/3}$ law and the influence of external turbulence is weak. In contrast, Rind & Castro (2012*a*) found a significantly faster decay of

U_0 when the external turbulence had levels similar to the $u'_{ext} = 3\,\%$ and $4\,\%$ cases considered here. The reasons for this difference are examined in the present section.

The primary independent parameters in the present problem are taken to be the level of external turbulence, u'_{ext}, the wake deficit velocity, U_0, and the wake turbulence, u'_{cl}, all obtained at the time when the combined wake is initialized. The resulting non-dimensional parameters are u'_{ext}/U_0 and u'_{ext}/u'_{cl}. As shown by Rind & Castro (2012*a*), the effect of external turbulence on the mean wake velocity strengthens when u'_{ext}/U_0 increases. We hypothesize that u'_{ext}/u'_{cl} is also important because of the following considerations. As discussed in § 4, it is the turbulent production, P, that is the dominant sink in (4.1), the transport equation for m.k.e. The Reynolds shear stress appearing in P is quadratic in velocity fluctuations. In the undisturbed wake, $P \propto u'^2$, where u' is the level of wake turbulence. External turbulence provides a turbulence reservoir that can maintain turbulence fluctuations in the wake by decreasing the transport of turbulence away from the wake and increasing shear production. The increase in P due to external fluctuations with level u'_{ext} can be estimated for the combined wake as

$$\delta P \approxeq \alpha_1 u' u'_{ext} + \alpha_2 {u'_{ext}}^2 \approxeq u'^2 \left(\alpha_1 \frac{u'_{ext}}{u'} + \alpha_2 \left(\frac{u'_{ext}}{u'} \right)^2 \right). \tag{7.1}$$

Our objective is to understand how the parameters related to mean and fluctuating velocity at the point of initialization of the combined wake change the subsequent evolution of the wake mean field. To do so, we assume that the change δQ in the cumulative integrated production, $Q = \int_0^t \int_C P \mathrm{d}C\mathrm{d}t$, which was introduced earlier, is solely due to δP and estimate u'_{ext}/u'_{cl} using initial values to give

$$\frac{\delta Q}{\text{t.k.e.}_0} \approxeq \beta_1 \frac{u'_{ext}}{u'_{cl}} + \beta_2 \left(\frac{u'_{ext}}{u'_{cl}} \right)^2. \tag{7.2}$$

In general, the coefficients β_1 and β_2 are not universal and, in particular, can depend on the state of development of the wake at the point of initialization of the combined wake. The arguments leading to (7.2) apply to stratified wakes too with the understanding that β_1 and β_2 depend additionally on Fr.

Rind & Castro (2012*a*) combine background fluctuations when the wake is in an approximately self-similar state ($t \approx 60$), while we do so in the near-wake region where the turbulent fluctuations are considerably stronger. Case RC4 (our nomenclature for their case with $u'_{ext}/U_0 = 0.36$) shown in table 2 has a value of u'_{ext}/U_0 similar to our original case $EXT4_{unst}$ where $u'_{ext}/U_0 = 0.4$. However, case RC4 has $u'_{ext}/u'_{\delta} = 1.25$, which is higher than the corresponding value of 0.87 in $EXT4_{unst}$. This higher level of external turbulence relative to wake turbulence, and the fact that β_1 and β_2 depend on the state of wake turbulence (self-similar in contrast to early time) during combination, is perhaps responsible for the substantially larger effect of external fluctuations found by Rind & Castro (2012*a*).

New cases with $Re = 10\,000$ are simulated to support the preceding arguments. In order to establish that u'_{cl} plays a role in how the wake evolution is affected by background fluctuations, new simulations (series 2) with the same U_0 as the original series 1 but with lower u'_{cl} are performed. A wake without external turbulence, $EXT0_{2,unst}$, and the same wake parameters as series 2 is also simulated so as to provide a baseline. In our original series 1 of unstratified wake simulations, the effect of external turbulence is found to be weak. This is somewhat surprising given (7.2)

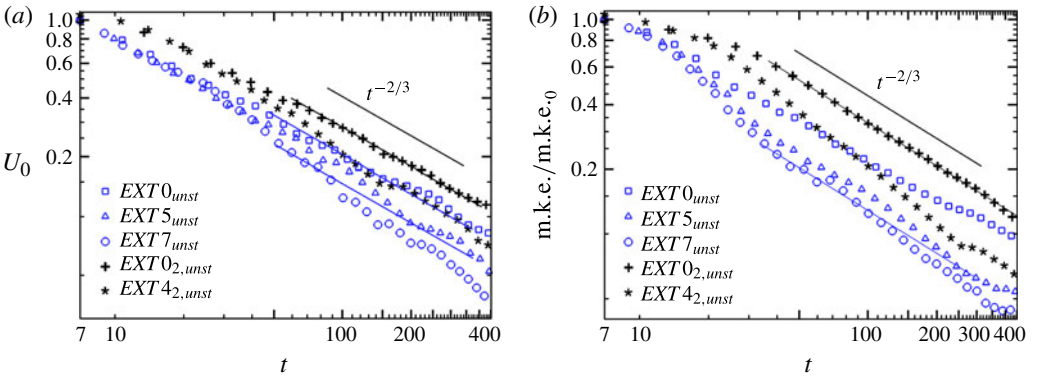

FIGURE 15. (Colour online) Effect of external fluctuations on mean wake velocity in unstratified wakes: (*a*) centre line defect velocity and (*b*) integrated mean kinetic energy.

Cases	U_0	u'_{cl}	u'_δ	u'_{ext}	$\frac{u'_{ext}}{U_0}$	$\frac{u'_{ext}}{u'_\delta}$	$\frac{u'_{ext}}{u'_{cl}}$
RC4	0.083	—	0.024	0.030	0.36	1.25	—
Series 1	0.1	0.044	0.047	0.01–0.072	0.10–0.72	0.22–1.53	0.23–1.64
Series 2	0.1	0.023	0.029	0.01–0.040	0.10–0.40	0.43–1.72	0.43–1.74

TABLE 2. Parameters relevant to the discussion of § 7 on the decay of the mean wake in unstratified flow. RC4 denotes a case from Rind & Castro (2012*a*). The velocities given in columns 2–5 are normalized with U, the free-stream velocity relative to the body. In order to compare with Rind & Castro (2012*a*) who use the r.m.s. velocity fluctuation at the wake half-width, u'_δ, to characterize wake turbulence, we give values of u'_δ in addition to u'_{cl}. Series 1 is the original series of simulations where $u'_{ext} = 1$–$4\,\%$ of U plus additional simulations with larger $u'_{ext} = 5\,\%$ and $7\,\%$. Series 2 is a new series where the wake has a lower level of centreline turbulence, $u'_{cl} = 2.3\,\%$, relative to the $4.4\,\%$ of series 1.

and the results reported by Rind & Castro (2012*a*). Therefore, we continue series 1 with two new cases where the external turbulence level is raised to $5\,\%$ and $7\,\%$ of the free-stream velocity.

Figure 15(*a*) shows that the case $EXT4_{2,unst}$ with $4\,\%$ external turbulence in the new series exhibits a substantial decrease in wake defect velocity relative to the uniform free-stream case $EXT0_{2,unst}$, while the original case with $EXT4_{2,unst}$ with $4\,\%$ external turbulence that was shown in figure 6(*a*) exhibited a small influence of external turbulence. This result supports the hypothesis that the wake turbulence level, u'_{cl}, plays an important role. It is also of interest to compare the new towed wake with $0\,\%$ external turbulence case, $EXT0_{2,unst}$, with the original $EXT0_{unst}$. Case $EXT0_{2,unst}$ has smaller u'_{cl}, leading to smaller turbulent production, smaller extraction of turbulence from the mean and, therefore, higher defect velocity relative to $EXT0_{unst}$. Nevertheless, both cases (particularly $EXT0_{2,unst}$) exhibit $U_0 \approx t^{-2/3}$ scaling that is anticipated from similarity theory of the far wake. In contrast to the small change of $U_0(t)$ in the $u'_{ext} = 4\,\%$ case of series 1, the new series 1 cases with $u'_{ext} = 5\,\%$ and $u'_{ext} = 7\,\%$ shown in figure 15(*a*) exhibit lower levels of $U_0(t)$ compared with the uniform free-stream case, consistent with the result of Rind & Castro (2012*a*) that, with increasing u'_{ext}, the decay of $U_0(t)$ is enhanced and deviates from the $t^{-2/3}$ law.

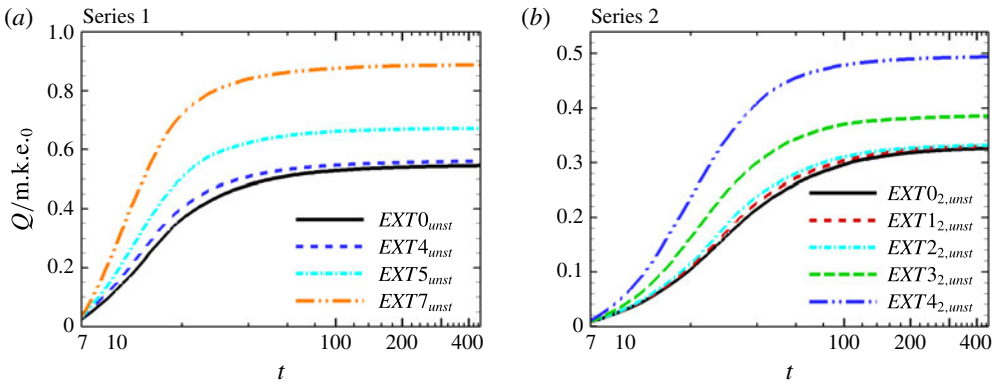

FIGURE 16. (Colour online) Cumulative area-integrated value of turbulent production normalized by the initial integrated mean kinetic energy. (*a*) Results from series 1 ($u'_{cl}/U_0 = 0.044$), (*b*) Results from series 2 ($u'_{cl}/U_0 = 0.023$).

The effect of external turbulence on the area-integrated m.k.e. (figure 15*b*) is similar to that on the defect velocity U_0. One difference is that the evolution of $U_0(t)$ deviates later than the m.k.e. from the corresponding uniform free-stream case, consistent with the expectation that the effect of external turbulence on wake dynamics needs time to propagate from the wake flanks to its core.

External turbulence affects the evolution of mean wake velocity by changing the turbulent production. Figures 16(*a*) and (*b*) show that the cases where the wake mean velocity is reduced by the presence of external turbulence also show an increase in cumulative turbulent production $Q(t)$. It can also be seen that the effect of external turbulence in increasing $Q(t)$ from the corresponding uniform free-stream case becomes significant at $u'_{ext} = 3\,\%$ in series 1 relative to $u'_{ext} = 5\,\%$ required in series 2.

The deviation of the external turbulence cases with respect to the baseline is quantified by the change, δQ_f, of the long-time value of Q_f (evaluated at $t \approx 450$) with respect to Q_f in the corresponding uniform free-stream case. The value of $\delta Q_f/\text{t.k.e.}_0$ depends strongly on u'_{ext}/u'_{cl} in both unstratified and stratified cases, as shown by figures 17(*a*) and 17(*b*) respectively. In the unstratified cases, there is little change in turbulent production (therefore, mean velocity evolution) until $u'_{ext}/u'_{cl} > 1$. Once the threshold of $u'_{ext}/u'_{cl} \approxeq 1$ is exceeded, there is strong transport of turbulence from the exterior into the wake, allowing δQ to increase sharply. Similar behaviour is also observed in the stratified cases with $Fr = 3$. The lines in figure 17(*a*,*b*) are best-fit curves of the quadratic function, (7.2), and provide a reasonable fit to the simulation data. It is worth noting that, in series 1, δQ_f takes small negative values when $u'_{ext}/u'_{cl} < 1$. In all cases, $P(t)$ is enhanced by external fluctuations during the early evolution, but, later, $P(t)$ is reduced because of the mean velocity feedback, i.e. the wake spread rate increases, decreasing the mean shear and, eventually, decreasing $P(t)$. In the cases with negative values of δQ_f (figure 17*a*), the late-time reduction of $P(t)$ dominates.

Upon normalization by Q_f, the effect of external turbulence becomes even more substantial, e.g. the $EXT4_{st}$ case in series 1, $Fr = 3$ with $u'_{ext}/u'_{cl} \approx 1$, has $\delta Q_f/Q_f = 0.14$, a higher value than the $\delta Q_f/\text{t.k.e.}_0 = 0.05$ in figure 17(*b*). Since Q_f is essentially the change in integrated m.k.e. for the clean wake without external turbulence, it is the

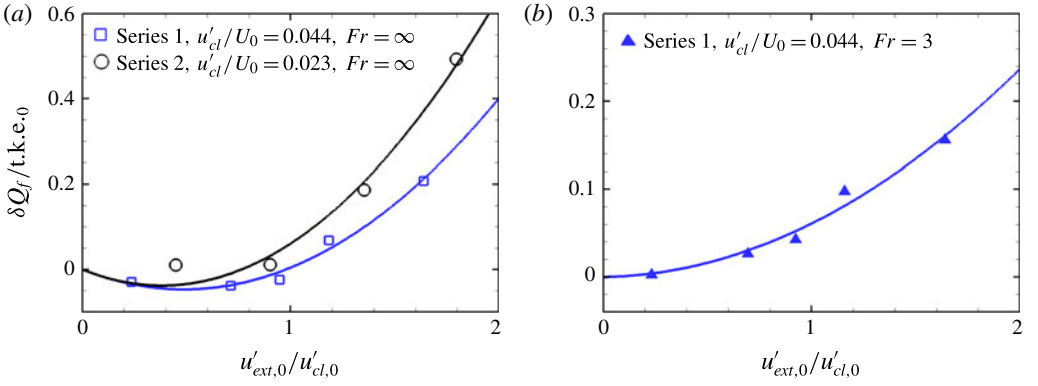

FIGURE 17. (Colour online) The influence of u'_{ext}/u'_{cl} at the initialization of the combined wake on the external turbulence effect: (*a*) unstratified cases, (*b*) stratified cases. Here, δQ_f, defined in the accompanying text, is a measure of the long-time deviation of a wake evolving in external turbulence with respect to a case without external turbulence in the same series.

value of $\delta Q_f/Q_f$ that effectively measures the relative deviation of the mean wake velocity from the clean wake evolution.

8. Conclusions

Towed wakes at $Re = 10\,000$ have been examined using DNS in a temporally evolving framework in order to study the influence of background turbulence on the evolution of wakes. Although simulations are conducted for both unstratified and stratified cases, the primary focus is on stratified wakes. The ratio of the integral length scale of the external background turbulence to that of the wake turbulence is $O(1)$. The r.m.s. intensity of the background turbulence, u'_{ext}, is systematically varied in the simulations. The effect of background turbulence is discussed using visualizations, turbulence statistics and analysis of the t.k.e. balance equation.

Background turbulence at 1 % has little effect on the spatial organization of the stratified wake except for one aspect: the spatial pattern of internal waves, an important feature characterizing stratified wakes, is disrupted even at this low turbulence level. However, the organization of horizontal motion into coherent pancake vortices, which is a defining characteristic of strongly stratified turbulence, is robust to the presence of external turbulence. Due to buoyancy, the decaying background fluctuations also organize into vortical structures which interact with the wake vortices leading to a larger lateral spread of the wake vortices. Horizontal x_1–x_2 cuts and vertical x_1–x_3 cuts of velocity and the vorticity normal to the plane show large-scale coherent structures. It is worth noting that, because the external fluctuations are also organized into pancake vortices, planar cuts of normal vorticity do not clearly show the presence of the late-time wake when the background turbulence is larger than or equal to 4 %. In contrast, planar cuts of the velocity show the presence of the late-time wake.

The evolution of the centreline defect velocity in all the stratified wake cases shows the different regimes, namely, NW, non-equilibrium (NEQ) and quasi-two-dimensional (Q2D), with their characteristic decay laws that have been found in several previous studies of wakes in a quiescent background. Despite the presence of external

turbulence, the centreline defect velocity remains substantially higher than the corresponding unstratified cases; that is, stratified wakes continue to have longer lifetimes.

External turbulence has an important effect on the mean defect velocity, $U_0(t)$. When u'_{ext} exceeds 3 % in the $Fr = 3$ cases, $U_0(t)$ eventually becomes substantially smaller relative to the uniform free-stream case. The turbulence production by shear also increases and the consequent enhancement of transfer from mean to turbulent kinetic energy leads to a decrease in mean velocity. The r.m.s fluctuation profiles also become wider in the lateral horizontal coordinate. There is little change in the vertical centreline profiles of mean and turbulence quantities, showing that the stabilizing effect of buoyancy remains dominant. The area-integrated turbulent kinetic energy becomes larger with increasing u'_{ext}.

External turbulence induces a faster decay of the mean wake in both unstratified and stratified wakes. For a given intensity of external turbulence, the stratified cases show a stronger relative change of mean velocity. The discussion of § 7 leads to the following conclusion. For both unstratified and stratified wakes, the parameter u'_{ext}/u'_{cl}, which measures the intensity of the external turbulence relative to the wake turbulence, is the key parameter that governs the influence of external fluctuations. There is a rapid increase in the cumulative turbulent production and, therefore, the mean wake decay when u'_{ext}/u'_{cl} exceeds a value of approximately unity. The present simulations were performed at $Re = 10\,000$. However, the finding that external turbulence with length scale similar to wake turbulence substantially affects the wake dynamics when $u'_{ext}/u'_{cl} > 1$ is expected to be true at larger values of Re. The dependence of the cumulative turbulent production at a late time ($t \approx 450$), and, therefore, the decay of area-integrated mean kinetic energy up to that time, was found to have an approximately quadratic dependence on u'_{ext}/u'_{cl} for the cases examined here. The parameters u'_{ext}/u'_{cl} and u'_{ext}/U_0 are varied independently in the simulations, and u'_{ext}/u'_{cl} is found to be the key governing parameter. If the external turbulence is added when the wake is already in its self-similar state (when the ratio of centreline r.m.s. velocity fluctuation to mean defect velocity is constant in time), as in the simulations of Rind & Castro (2012*a*), then u'_{ext}/U_0 and u'_{ext}/u'_{cl} are not independent parameters.

Future work will be necessary to determine whether our finding of $u'_{ext}/u'_{cl} > 1$ as a criterion for external turbulence to substantially change the mean wake velocity carries over to other background configurations. The relative value of the turbulence integral scale, $l_{int,ext}/l_{int,cl}$, was $O(1)$ in both the present study and that by Rind & Castro (2012*a*). Larger and smaller values of this ratio could be the subject of future study. The external turbulence chosen in the present work is isotropic turbulence that decays along with the wake. This simplified case is similar to that in wind tunnel experiments of a wake with grid turbulence providing the background fluctuations. It is possible that, if the background turbulence exhibited a much slower decay than the wake turbulence, its effect on the wake would be stronger. The complexity of the flow behind the body where the external turbulent background mixes with the separating boundary layers and the NW is not included in the present simulations. Therefore, future investigations that include the body will help to evaluate the role of NW dynamics on the effect of external turbulence on the intermediate to far wake.

Acknowledgements

We gratefully acknowledge the support of ONR grant no. N0014-11-10469 administered by Dr R. Joslin. Computational resources were provided by the

Department of Defense High Performance Computing Modernization Program. We would also like to thank the three anonymous referees whose helpful suggestions improved the quality of this paper.

REFERENCES

ABDILGHANIE, A. M. & DIAMESSIS, P. J. 2013 The internal gravity wave field emitted by a stably stratified turbulent wake. *J. Fluid Mech.* **720**, 104–139.

AMOURA, Z., ROIG, V., RISSO, F. & BILLET, A.-M. 2010 Attenuation of the wake of a sphere in an intense incident turbulence with large length scales. *Phys. Fluids* **22**, 055105.

BAGCHI, P. & BALACHANDAR, S. 2004 Response of the wake of an isolated particle to an isotropic turbulent flow. *J. Fluid Mech.* **518** (1), 95–123.

BAZILEVS, Y., YAN, J., DESTADLER, M. & SARKAR, S. 2014 Computation of the flow over a sphere at $Re = 3700$: a comparison of uniform and turbulent inflow conditions. *Trans. ASME J. Appl. Mech.* **81**, 121003.

BEVILAQUA, P. M. & LYKOUDIS, P. S. 1978 Turbulence memory in self-preserving wakes. *J. Fluid Mech.* **89** (3), 589–606.

BONNETON, P., CHOMAZ, J. M., HOPFINGER, E. & PERRIER, M. 1996 The structure of the turbulent wake and the random internal wave field generated by a moving sphere in a stratified fluid. *Dyn. Atmos. Oceans* **23** (1), 299–308.

BONNETON, P., CHOMAZ, J. M. & HOPFINGER, E. J. 1993 Internal waves produced by the turbulent wake of a sphere moving horizontally in a stratified fluid. *J. Fluid Mech.* **254**, 23–40.

BONNIER, M. & EIFF, O. 2002 Experimental investigation of the collapse of a turbulent wake in a stably stratified fluid. *Phys. Fluids* **14**, 791–801.

BRUCKER, K. A. & SARKAR, S. 2007 Evolution of an initially turbulent stratified shear layer. *Phys. Fluids* **19**, 105105.

BRUCKER, K. A. & SARKAR, S. 2010 A comparative study of self-propelled and towed wakes in a stratified fluid. *J. Fluid Mech.* **652**, 373–404.

CHOMAZ, J. M., BONNETON, P. & HOPFINGER, E. J. 1993*a* The structure of the near wake of a sphere moving horizontally in a stratified fluid. *J. Fluid Mech.* **254** (1), 1–21.

DIAMESSIS, P. J., SPEDDING, G. R. & DOMARADZKI, J. A. 2011 Similarity scaling and vorticity structure in high Reynolds number stably stratified turbulent wakes. *J. Fluid Mech.* **671**, 52–95.

DOMMERMUTH, D. G., ROTTMAN, J. W., INNIS, G. E. & NOVIKOV, E. A. 2002 Numerical simulation of the wake of a towed sphere in a weakly stratified fluid. *J. Fluid Mech.* **473**, 83–101.

GHOSAL, S. & ROGERS, M. M. 1997 A numerical study of self-similarity in a turbulent plane wake using large-eddy simulation. *Phys. Fluids* **9** (6), 1729–1739.

GILREATH, H. E. & BRANDT, A. 1985 Experiments on the generation of internal waves in a stratified fluid. *AIAA J.* **23** (5), 693–700.

GOURLAY, M. J., ARENDTH, S. C., FRITTS, D. C. & WERNE, J. 2001 Numerical modeling of initially turbulent wakes with net momentum. *Phys. Fluids* A **13**, 3783–3802.

LEGENDRE, D., MERLE, A. & MAGNAUDET, J. 2006 Wake of a spherical bubble or a solid sphere set fixed in a turbulent environment. *Phys. Fluids* **18**, 048102.

LIN, J. T. & PAO, Y. H. 1979 Wakes in stratified fluids. *Annu. Rev. Fluid Mech.* **11**, 317–338.

MEUNIER, P. & SPEDDING, G. R. 2006 Stratified propelled wakes. *J. Fluid Mech.* **552**, 229–256.

MOSER, R. D., ROGERS, M. M. & EWING, D. W. 1998 Self-similarity of time-evolving plane wakes. *J. Fluid Mech.* **367**, 255–289.

PAL, A., DE STADLER, M. B. & SARKAR, S. 2013 The spatial evolution of fluctuations in a self-propelled wake compared to a patch of turbulence. *Phys. Fluids* **25**, 095106.

REDFORD, J. A., CASTRO, I. P. & COLEMAN, G. N. 2012 On the universality of turbulent axisymmetric wakes. *J. Fluid Mech.* **710**, 419–452.

REDFORD, J. A. & COLEMAN, G. N. 2007 Numerical study of turbulent wakes in background turbulence. In *5th International Symposium on Turbulence and Shear Flow Phenomena (TSFP-5 Conference), Munich, Germany*, pp. 561–566.

RIND, E. & CASTRO, I. P. 2012*a* Direct numerical simulation of axisymmetric wakes embedded in turbulence. *J. Fluid Mech.* **710**, 482–504.

RIND, E. & CASTRO, I. P. 2012*b* On the effects of free-stream turbulence on axisymmetric disc wakes. *Exp. Fluids* **53** (2), 301–318.

RODRIGUEZ, I., BORELLI, Y., LEHMKUHL, O., PEREZ SEGARRA, C. D. & ASSENSI, O. 2011 Direct numerical simulation of the flow over a sphere at $Re = 3700$. *J. Fluid Mech.* **679**, 263–287.

SPEDDING, G. R., BROWAND, F. K. & FINCHAM, A. M. 1996*a* The long-time evolution of the initially turbulent wake of a sphere in a stable stratification. *Dyn. Atmos. Oceans* **23** (1–4), 171–182.

DE STADLER, M. B. & SARKAR, S. 2012 Simulation of a propelled wake with moderate excess momentum in a stratified fluid. *J. Fluid Mech.* **692**, 28–52.

UBEROI, M. S. & FREYMUTH, P. 1970 Turbulent energy balance and spectra of axisymmetric wake. *Phys. Fluids* **13** (9), 2205–2210.

WU, J.-S. & FAETH, G. M. 1994 Sphere wakes at moderate Reynolds numbers in a turbulent environment. *AIAA J.* **32** (3), 535–541.

WU, J.-S. & FAETH, G. M. 1995 Effect of ambient turbulence intensity on sphere wakes at intermediate Reynolds number. *AIAA J.* **33** (1), 171–173.